



Water-Soluble Non-Ionic PEGylated Porphyrins: A Versatile Category of Dyes for Basic Science and Applications

Valentina Villari¹ · Norberto Micali¹ · Angelo Nicosia² · Placido Mineo^{1,2}

Received: 9 April 2021 / Accepted: 28 July 2021

© The Author(s), under exclusive licence to Springer Nature Switzerland AG 2021

Abstract

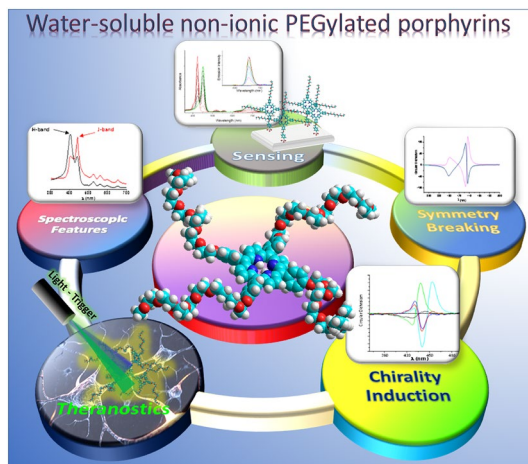
This review arises from the need to rationalize the huge amount of information on the structural and spectroscopic properties of a peculiar class of porphyrin derivatives—the non-ionic PEGylated porphyrins—collected during almost two decades of research. The lack of charged groups in the molecular architecture of these porphyrin derivatives is the leitmotif of the work and plays an outstanding role in highlighting those interactions between porphyrins, or between porphyrins and target molecules (e.g., hydrophobic-, hydrogen bond related-, and coordination-interactions, to name just a few) that are often masked by stronger electrostatic contributions. In addition, it is exactly these weaker interactions between porphyrins that make the aggregated forms more prone to couple efficiently with external perturbative fields like weak hydrodynamic vortexes or temperature gradients. In the absence of charge, solubility in water is very often achieved by covalent functionalization of the porphyrin ring with polyethylene glycol chains. Various modifications, including of chain length or the number of chains, the presence of a metal atom in the porphyrin core, or having two or more porphyrin rings in the molecular architecture, result in a wide range of properties. These encompass self-assembly with different aggregate morphology, molecular recognition of biomolecules, and different photo-physical responses, which can be translated into numerous promising applications in the sensing and biomedical field, based on turn-on/turn-off fluorescence and on photogeneration of radical species.

✉ Valentina Villari
villari@ipcf.cnr.it

¹ IPCF-CNR, Istituto per i Processi Chimico-Fisici, Viale F. Stagno d'Alcontres 37, 98158 Messina, Italy

² Dipartimento di Scienze Chimiche, Università di Catania, Viale Andrea Doria 6, 95125 Catania, Italy

Graphic Abstract



Keywords PEGylated porphyrins · Self-assembly · Supramolecular chirality · Optical properties · Mesoscopic structures

1 Introduction

Porphyrins are undoubtedly one of the most investigated classes of dyes. The scientific interest they have excited from the very beginning arises from their optical properties, namely very high molar extinction coefficient in the visible region and fluorescence quantum yield. The former helped to understand, for example, the effect of the exciton coupling mechanism on the degenerate (or quasi-degenerate) main absorption band of the molecule during aggregation, as well as the chirality transfer phenomenon upon interaction with biomolecules or nucleic acids. In addition, the strong electronic coupling between porphyrins in a supramolecular aggregate represented the basic model for the study of antenna systems and energy conversion devices [1–5]. The strong fluorescence, on the other hand, was frequently exploited to monitor the interaction with membranes and to study the confinement in the microenvironment of micelles and liposomes as a model of cell membranes.

Easy coordination with metals in the molecule core and covalent functionalization of the peripheral groups (for a recent review, see [6]), even with rather complex molecules, extend the range of electronic and optical properties of the porphyrins and their mechanisms of interaction with other species [7, 8].

More recently, the scientific community has been turning much attention to the study of porphyrins exploitable in photodynamic therapy against solid tumors [9] or in the sensor field as “turn off–on” fluorescence sensors of chemical species (e.g., pollutants like heavy metals and pesticides) [10–12]. Indeed, the photosensitizer action of porphyrins, namely the ability to produce reactive oxygen radicals

(superoxide, hydrogen peroxide, hydroxyl radicals, etc.) when irradiated at the proper wavelength, is the basic process used to induce toxicity in cells in the treatment of some kinds of cancer. Therefore, the main aim of current research in this field is to confer selectivity to porphyrin towards the cells of tumor tissues by functionalizing the molecular structure with specific receptors.

With regard to porphyrin as a fluorescence sensor, many works have been based on the ability of porphyrin in solution to form energy or electron donor/acceptor systems with a substrate or nanoparticle (through supramolecular interaction), which leads to significant quenching of the fluorescence signal of porphyrin. If the interaction with the target molecule, added to the solution, perturbs the supramolecular complex up to separation, porphyrin fluorescence tends to be restored. A certain degree of specificity in the interaction with the target molecule would give more selectivity to the sensor also in this case.

The main limitation in application of these dyes lies in the poor solubility in water of non-ionic species and the predominance of the electrostatic contribution from ionic species, which prevents specific interaction with target molecules from emerging. In the last two decades, efforts to overcome these drawbacks produced a huge variety of water-soluble macromolecular architectures derived from porphyrins, many of them devoid of chargeable groups but possessing water-soluble polymer chains linked covalently to all or some of the peripheral positions of the porphyrin macrocycle. More sophisticated architectures even encompass dendritic structures and molecular cages.

The choice of polymer to link is determined strictly by the properties the porphyrin derivative is expected to have. Chains can be thermo-responsive, drive aggregation phenomena for drug inclusion through hydrophilic/hydrophobic balance, possess biocompatibility and exhibit stealth effects with regards to the immune system. The latter property is the most frequently considered for perspective in biomedical applications such as photodynamic therapy, but is also extremely useful for investigating the role of hydrophobic interactions, hydrogen bonds, and coordination in the absence of charged groups, both between porphyrins and between porphyrins and target molecules. It exploits the high solubility in water of polyethylene glycol (PEG) chains, its biocompatibility and the fact that the porphyrin optical properties remain almost unaffected by PEG.

The interest in this class of PEG-modified porphyrins, named PEGylated porphyrin derivatives, is lively and growing. Thus, this review was inspired by the need to rationalize the huge amount of information on the structural and spectroscopic properties of PEGylated porphyrin derivatives, along with knowledge on their supramolecular binding with target molecules, nanoparticles or substrates, collected during almost two decades of research activity. The lack of charged groups in the molecular architecture and the solubility in water of these porphyrin derivatives is the key element of this review, in which each section is devoted to one characteristic aspect, common to the class, and presented with the related literature. In particular, after a brief recap of the main properties of the porphyrin macrocycle, useful for understanding the spectral response to photoexcitation, there are sections on (i) macromolecular architecture, self-assembly and resulting aggregate morphology; (ii) chirality transfer and molecular recognition of biomolecules; (iii) generation of phototoxic

species with perspectives in photodynamic therapy; and (iv) binding to target molecules or atoms for applications in the imaging or sensor field.

These topics, despite being the most prolific in terms of experimental works and published articles regarding PEGylated porphyrins, have no pretension to be an exhaustive review of all the features and potentiality of such compounds, but aim to furnish an outline of useful information for interested readers and act as a starting point for rousing the interest of those less expert in this field.

2 Porphyrin Spectroscopic Features

The overall profile of the absorption spectrum of porphyrin derivatives depends basically on macrocycle singlet energy levels. The profile displays a main band—the B or Soret band—corresponding to the S_0 – S_2 electronic transition (typically in the wavelength region of ~410–430 nm) and two or four weaker bands—Q bands—depending on the macrocycle symmetry related to the S_0 – S_1 transitions (typically in the wavelength region of ~450–660 nm). In the free-base porphyrin, the transition dipole moment associated with the electron promoted from S_0 to S_2 is represented by two quasi-degenerate transitions B_x and B_y (see Fig. 1a), which,

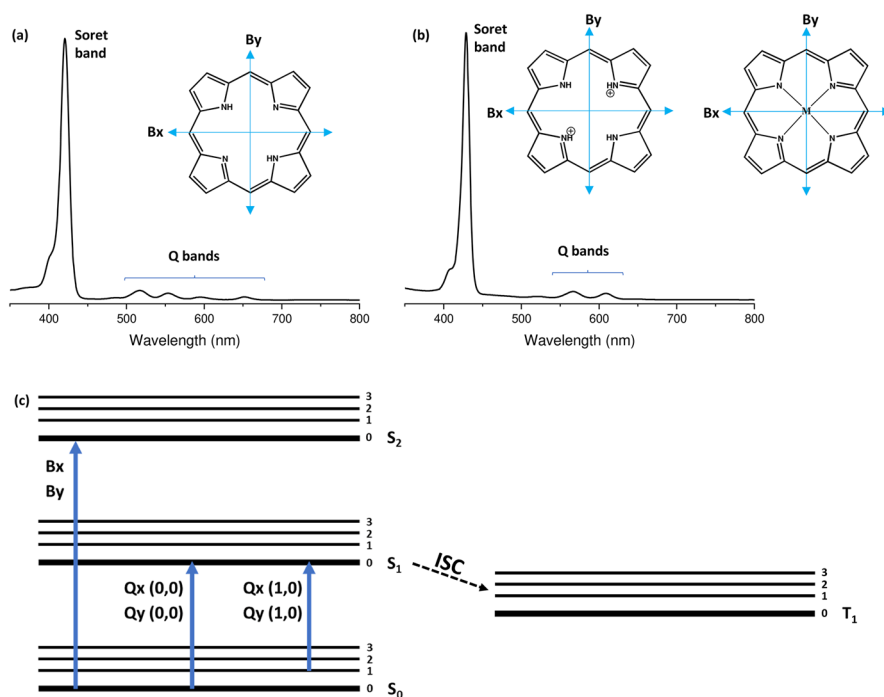


Fig. 1 Sketch of the transitions of **a** free-base and **b** diacid or metal porphyrin with the corresponding representative absorption spectrum. **c** Scheme of energy levels in electronic transitions during light absorption. *Dashed arrow* Inter-system crossing (ISC) from the singlet to the triplet state

due to symmetry, become degenerate when the core is protonated or a coordination metal is present (Fig. 1b).

Likewise, the transition dipole moments related to excitation from S_0 to S_1 are described by Q_x and Q_y , which are degenerate for the protonated or metal-coordinated porphyrin core. Within these transitions, different vibrational levels [$Q_x(0,0)$, $Q_x(1,0)$, $Q_y(0,0)$ and $Q_y(1,0)$] are involved, as depicted in Fig. 1c. Therefore, in the case of the free-base porphyrin, the degeneracy of the B transition is not resolved in the absorption spectrum, but is for the Q transitions, so that four bands appear instead of two.

The absorption spectrum of porphyrins has long been understood in terms of the “four-orbital” model (two highest occupied π orbitals, HOMO, and two lowest unoccupied π^* orbitals, LUMO) discussed by Gouterman [13, 14].

As far as fluorescence emission is concerned, the steady-state spectrum is constituted by two bands (in the range 600–800 nm) due to the photons emitted during spontaneous de-excitation from S_1 to S_0 , the de-excitation from S_2 to S_1 being non-radiative. The total lifetime of the singlet excited state differs from species to species, depending also on the possible presence of a metal in the porphyrin core, but, generally, varies from fractions of a nanosecond to a few nanoseconds.

Porphyrins in the excited S_1 state can also undergo a spin conversion to the first triplet state T_1 (the inter-system crossing process sketched in Fig. 1c), especially when heavy coordination metals, e.g., platinum or palladium, are present [15–19]. Phosphorescence (with typical lifetimes from a few microseconds to tens of microseconds) is emitted upon de-excitation from T_1 to S_0 , and, despite being forbidden in principle, occurs in these porphyrins with a discrete quantum yield.

The features described above characterize the wide variety of porphyrins; functionalization with PEG chains (regardless of number and length) does not affect them significantly if porphyrin is in the monomeric form, as is the case, for example, in many organic solvents. Conversely, in water, if the PEG length is too short or the number of chains linked is small, self-assembly occurs.

From a general point of view, aggregation of dyes involves coupling between the transition dipole moments of the constituent monomers (exciton coupling) and, depending on their alignment, gives rise to specific changes in the absorption spectrum. If the arrangement of dyes in the aggregate allows the transition dipole moments to align in a slipped (head-to-tail) manner, very efficient coupling and exciton delocalization involving even tens of monomers is favored. According to Kasha [20], and following exciton coupling theory, these structures, known as J-type aggregates, are characterized by the appearance of a red-shifted absorption band with respect to that of the monomer (Fig. 2a). An important consequence of exciton delocalization is the peculiar narrow shape of this absorption band, which gives the large resonant enhancement of the scattered light [21, 22].

On the other hand, a face-to-face alignment of transition dipole moments in the aggregate gives rise to structures known as H-type, revealed by the presence of a blue-shifted absorption band (Fig. 2b). Although the resonance effects are less intense for H-aggregates than for J-aggregates, it is more pertinent to refer to both bands as extinction bands (absorption + scattering).

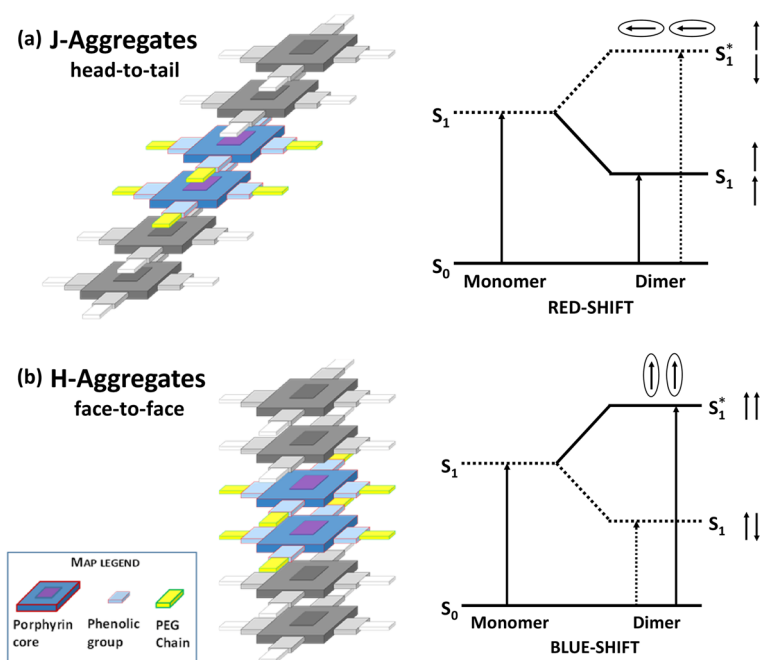


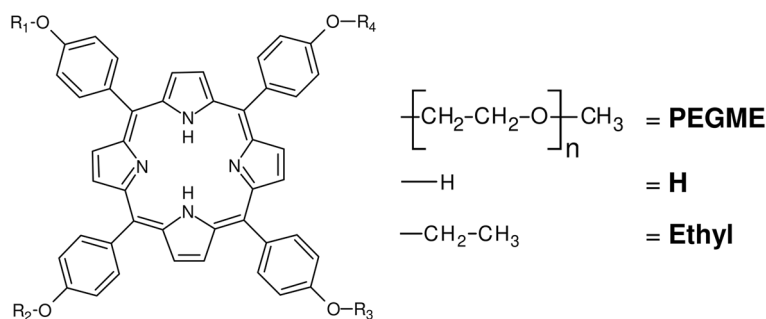
Fig. 2 Porphyrin alignment (*left*) and energy splitting (*right*) of allowed (*solid lines*) and forbidden (*dotted lines*) states according to exciton coupling theory for **a** J-type and **b** H-type aggregates

It is noteworthy that, due to the existence of two transitions (B_x and B_y), the aggregates of porphyrins and their derivatives usually display both H- and J-bands in the absorption spectrum, even if with very different amplitudes. Indeed, even if the aggregate grows preferentially along either the head-to-tail or face-to-face direction, thus displaying the related band as a main contribution, a certain degree of coupling occurs also in the perpendicular direction. Finally, the effect of exciton coupling on the emission properties of porphyrin aggregates is a significant quenching phenomenon.

In this context, PEGylated porphyrins are useful for understanding how to pilot the formation of each kind of aggregate, as described in the next section.

3 Design of Macromolecular Architecture and Resulting Aggregate Structures

The structural and conformational properties of self-assembled PEGylated porphyrins can be modulated by the appropriate design of the molecular architecture. The stacking phenomenon, steric hindrance, aggregate rigidity, hydrophobic/hydrophilic balance and the tendency to form hydrogen bonds can be varied by changing the peripheral positions and the number or length of PEG branches in the porphyrin macrocycle peripheral positions (Fig. 3).



Sample	R ₁	R ₂	R ₃	R ₄	n
1	PEGME	Ethyl	PEGME	Ethyl	17
2	PEGME	PEGME	H	H	17
3	PEGME	H	PEGME	H	17
4	PEGME	H	H	H	7
5	PEGME	PEGME	PEGME	H	3
6	PEGME	PEGME	PEGME	H	9
7	PEGME	PEGME	PEGME	H	17
8	PEGME	PEGME	PEGME	PEGME	9
9	PEGME	PEGME	PEGME	PEGME	17

Fig. 3 Examples of some molecular architectures of polyethylene glycol (PEG)-modified (PEGylated) porphyrin derivatives obtained from the tetra-hydroxyphenyl porphyrin macrocycle (n , polymerization degree of the PEG chain). *Table* Details of the molecular structures of the main PEGylated porphyrin derivatives

At low concentration (typically a few micromoles per liter), the triggering and extent of self-assembly depend crucially on the number of PEG chains and their length. If PEG is linked to all four peripheral positions of the macrocycle (star-like and dendritic molecular architecture), there is a threshold value of chain length below which molecules aggregate spontaneously in water because the polymer hydrophilicity is not sufficient to compensate for the strong hydrophobic character of the core [18, 23–28]. The influences of the thermodynamic conditions have also been investigated [29]. If less than four peripheral positions are involved, the increase in chain length can be insufficient to avoid aggregation [25, 30–37]. In this case, solubility in water can be achieved by linking two or more PEG chains to the same point [38].

The stacking of non-ionic PEGylated porphyrins is driven by hydrophobic and π - π interactions, with a non-negligible role of the hydrogen bond. The most common structure obtained in aqueous solution is represented by J-type aggregates [23, 25], which resemble many other porphyrins, but the position of the PEG chains and the absence of groups able to form intermolecular hydrogen bond definitely favor the formation of H-type aggregates [31, 39], as displayed schematically in Fig. 4.

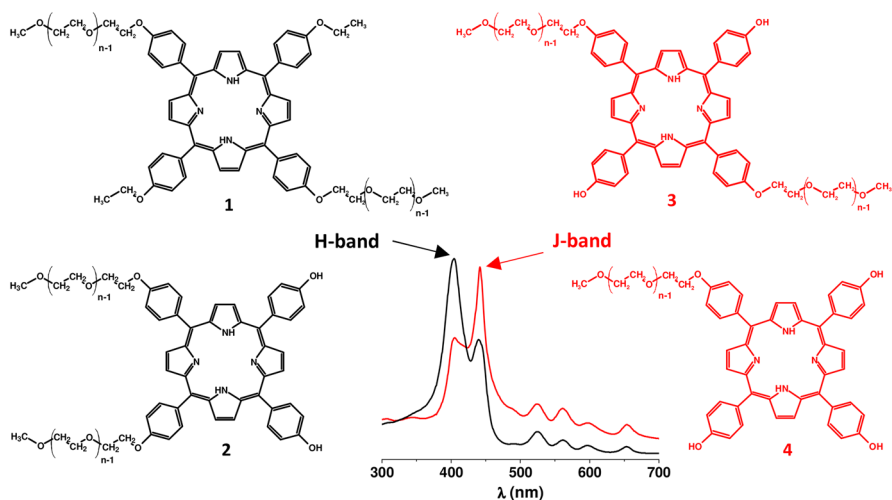


Fig. 4 The position and number of PEG chains in the porphyrin macrocycle, as well as the presence of groups able to stabilize the structure by forming hydrogen bonds, determine the geometrical arrangement during aggregation [30, 31, 39]. For details of the molecular structures of PEGylated porphyrin derivatives, see Fig. 3

The occurrence of either J- or H-aggregates becomes clearer from geometrical considerations on the mutually orthogonal transition dipole moments associated with the transitions B_x and B_y (Fig. 5).

The interaction energy is the value of the (red- or blue-) energy shift of the B_x and B_y transitions of the interacting porphyrins with respect to the porphyrin monomer, measured by the absorption spectrum. In the simpler case of perfectly parallel macrocycles (for which it holds $\alpha_1 = \alpha_2 = 0$, see Fig. 5), only the state corresponding to in-phase transition moment alignment is allowed from exciton theory (see Fig. 2); otherwise the excited state with out-of-phase transition dipole moments can also be populated, although with low probability, as it occurs more reasonably in real aggregates. Figure 5 summarizes the cases discussed.

By minimizing the steric hindrance in their mutual approach, and in the drive towards different aggregate types, the cis- (5,10-) or trans-positions (5,15-) of two PEG chains, for example, then play a decisive role in determining the geometrical parameters and the relative orientation of the macrocycles. Analogously, for star-like architectures (PEG chains in 5-,10-,15-,20- positions) the four PEG branches are too bulky to allow face-to-face alignment, so the head-to-tail arrangement (J-type) is preferred in the final structure of the aggregate. Finally, PEG position and length being the same, the energetically favored structure (more stable and more rigid) is the one allowing for the formation of hydrogen bonds between porphyrins [31, 39].

Another important consequence is the size of the final aggregate. The face-to-face arrangement of the H-type structure is more effective than the J-type in self-shielding the hydrophobic cores from water, so stability is reached at smaller aggregate size. In the J-type porphyrin alignment, the core surface exposed to the solvent

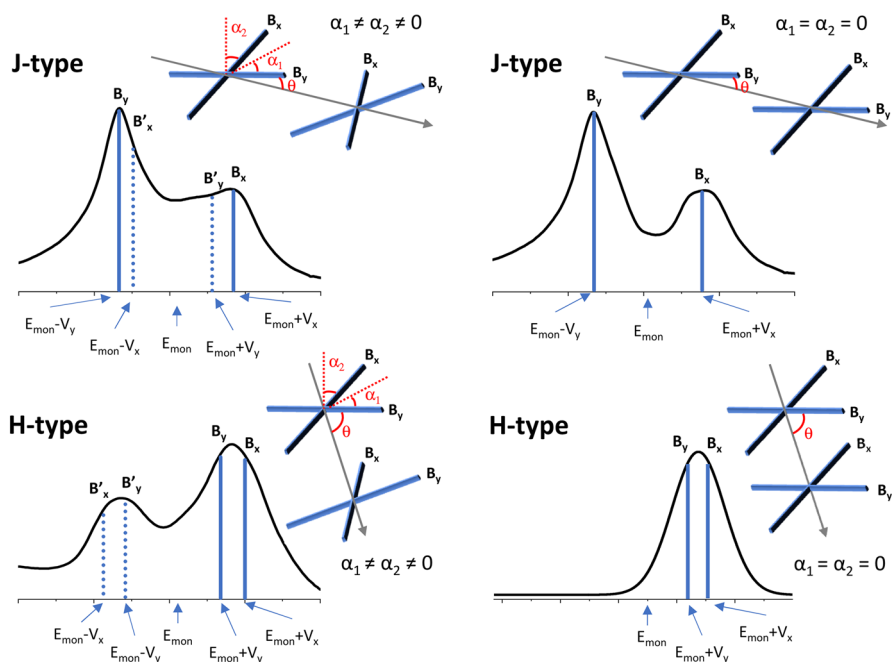


Fig. 5 Main geometrical characteristics of the porphyrin arrangement in the aggregate and corresponding energy profile of the absorption spectrum. $\vec{\mu}_x$ and $\vec{\mu}_y$ indicate the mutually orthogonal transition dipole moments associated with the transitions B_x and B_y ; any linear combination of them is equivalent [40]. Therefore, any direction of $\vec{\mu}_x$ and $\vec{\mu}_y$ in the ring plane of two interacting adjacent porphyrins is also equivalent, provided that they remain mutually orthogonal. Thanks to this symmetry, according to exciton coupling within the point dipole approximation [40, 41] the interaction energy between the transition dipole moments of two interacting porphyrins can be written as: $V_y = \frac{\mu^2}{R^3} [\cos \alpha_1 - 3 \cos \theta \cos (\theta - \alpha_1)]$ and $V_x = \frac{\mu^2}{R^3} \cos \alpha_2$, where R is the center-to-center dipole distance, α_1 and α_2 represent the angle between the $\vec{\mu}_y$ transition moments of the two interacting porphyrins and the angle between the $\vec{\mu}_x$ ones, respectively, in the general case of non parallel porphyrin macrocycles, and θ is the angle between $\vec{\mu}_y$ of the first porphyrin and the direction of R . By following the classification of Kasha, an aggregate is considered J-type when $\theta < 55^\circ$ and H-type for $\theta > 55^\circ$

is generally so wide that the strong π - π interaction contribution drives the formation of large, nearly micrometric, aggregates (even fractal-like) [31, 39].

The case of covalent dimeric, trimeric or n -meric porphyrin forms (cyclic architecture) deserves a mention (Fig. 6).

In the architectures provided by the PEGylated porphyrin derivative in cis- positions (Fig. 6a), the region occupied by the planar porphyrin core is even larger, causing very extended aggregation with more than micrometric size. For dimeric and trimeric forms (samples **10**, **11**) no precipitation is observed provided that the concentration is low and structure is not compact (as in fractals) [31]. For higher cyclic forms (samples **13**, **14**), solubility in water is obtained more easily by giving up the planar molecular architecture and using the porphyrin derivative that is PEGylated in trans- positions (Fig. 6b) to design a nano-box in which porphyrin cores can shield one another efficiently [42]. The nano-box molecular architecture

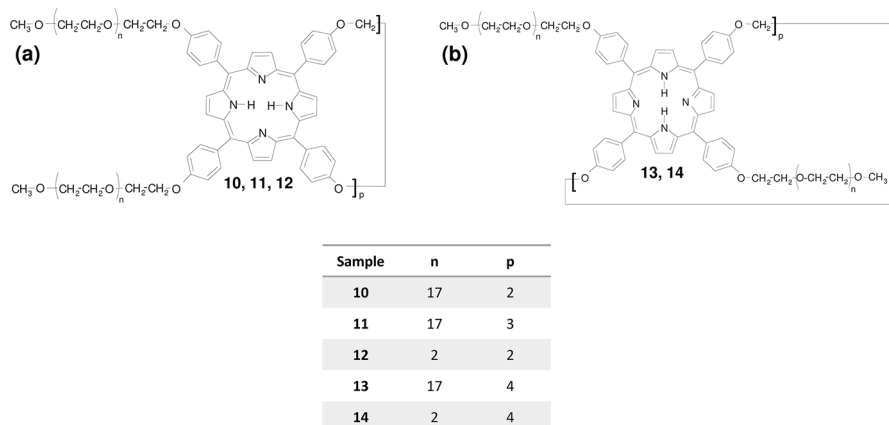


Fig. 6 a,b Molecular architectures of cyclic n -meric PEGylated porphyrin derivatives 5,10-di[p -(ω -methoxypolyethyleneoxy)phenyl]-15,20-di[p -oxyphenyl]porphyrin-formal (a) and 5,15-di[p -(ω -methoxypolyethyleneoxy)phenyl]-10,20-di[p -oxyphenyl]porphyrin-formal (b)

influences the electron density distribution of the macromolecule, as an effect of the interactions of π orbitals of the four-porphyrin cycle [43].

As mentioned above, often one or two PEG chains do not guarantee water solubility of porphyrin in the molecular form; rather, these kinds of architecture are properly designed to emphasize the separation between the hydrophobic and hydrophilic parts, so triggering the formation of nanoparticles (micelle-like) [32, 34, 37, 44–47]. Porphyrins constitute the inner part of the nanoparticle, in which macrocycles interact with one another in a face-to-face fashion. Nevertheless, the nanoparticle geometry does not allow for an extended exciton delocalization and the relative H-band is not very pronounced in the absorption spectrum [37, 46, 47]. PEGylated porphyrin nanoparticles have been investigated as biocompatible carriers of hydrophobic drugs into cells [32, 37]. They can be made even more versatile by using PEG as a copolymer of other polymeric species with pH- or thermo-responsive properties, useful for detecting environmental conditions in target tissues or in solution [44, 45].

4 Chirality Induction

Porphyrins are achiral and do not show any circular dichroism (CD) spectrum (they are CD silent), unless properly modified with groups possessing specific chiral centers. Nevertheless, they are able to interact with a huge variety of chiral species and to change their well-defined physico chemical properties in a definite and measurable way. The literature is very rich in studies about achiral porphyrins displaying, in the Soret region, an induced CD (ICD) signal by chiral templates supramolecularly bonded to them. The high molar extinction coefficient of porphyrins in the visible range makes them particularly sensitive for monitoring host–guest interactions and the mechanism of binding. In addition, obtaining chirality induction on porphyrin

aggregates during, or even after, the aggregation process is a powerful tool for amplifying the chiral signal and, consequently, the sensitivity of the system. These aspects will be considered here exclusively for uncharged PEGylated porphyrins in water, which disclose further information with respect to porphyrin molecules in general.

The ICD response changes in a recognizable way depending on the kind of bonded species. For example, provided that an appropriate metal atom is in the porphyrin core acting as ligand, binding with aliphatic and aromatic amino acids (Fig. 7a, sample 15) gives rise to different ICD signals [48]; other specific profiles are observed upon binding with different proteins [49]. A tweezer conformation can make the system even more selective, with different signs of ICD (as sketched in Fig. 7b, samples 16–18) also varying the bridge length and flexibility [50, 51].

Unlike in organic solvent, it was found that the same aromatic amino acids can bind to these PEGylated porphyrin tweezers through different arrangements: via coordination of one central metal atom of one porphyrin, the other porphyrin being not coordinated, or via coordination of one central metal atom and hydrophobic and/or π - π interactions of aromatic groups with the other porphyrin of the tweezers. Although it was observed that water molecules can compete for metal coordination and that the interacting species, especially amino acids, are water soluble in a rather wide pH range, the formation of stable supramolecular complexes is energetically favored [50].

Not only do the described properties underline the potential usefulness of PEGylated porphyrins as selective molecular sensors of amino acids and proteins directly in aqueous solution, they also help understand if, and to what extent, the exciton coupling approach is applicable in the split type ICD. In fact, it was proposed that the coupling between the magnetic ($n \rightarrow \pi^*$) and electric ($\pi \rightarrow \pi^*$) transition moments of the amino acid and the electric transition of the porphyrin can give different rotational strengths for not exactly degenerate B_x and B_y transitions (for instance, in the case of slight molecular asymmetry) [50].

Another stimulating topic is the emergence of chirality in supramolecular aggregates constituted by achiral building blocks. This phenomenon can occur only by means of external chemical or physical asymmetric perturbations: the use of chiral templates during the aggregation, asymmetric photosynthesis and photolysis caused by the irradiation with circularly polarized light, heterogeneous catalysis, and asymmetric fields. Achiral porphyrins have been exploited for studying the effect of asymmetric physical perturbation on their supramolecular aggregates, and many studies have involved the application of such a field from the very beginning of the aggregation kinetics. For example, consider the pioneering work on the effect of the hydrodynamic flux (vortex) [52, 53] or more recent results on the combined rotation and gravity in the presence of a magnetic field [54]. Strong hydrodynamic vortices, however, were shown to affect the distribution of enantiomers or enrichment in a solution of J aggregates already formed [55].

Also in this ambit, PEGylated porphyrins display new findings and peculiarities. The most impressive evidence came from the reversible chiral response induced on already formed achiral aggregates by a weak asymmetric perturbation. It was demonstrated that the switch-on of a weak thermal force (generated

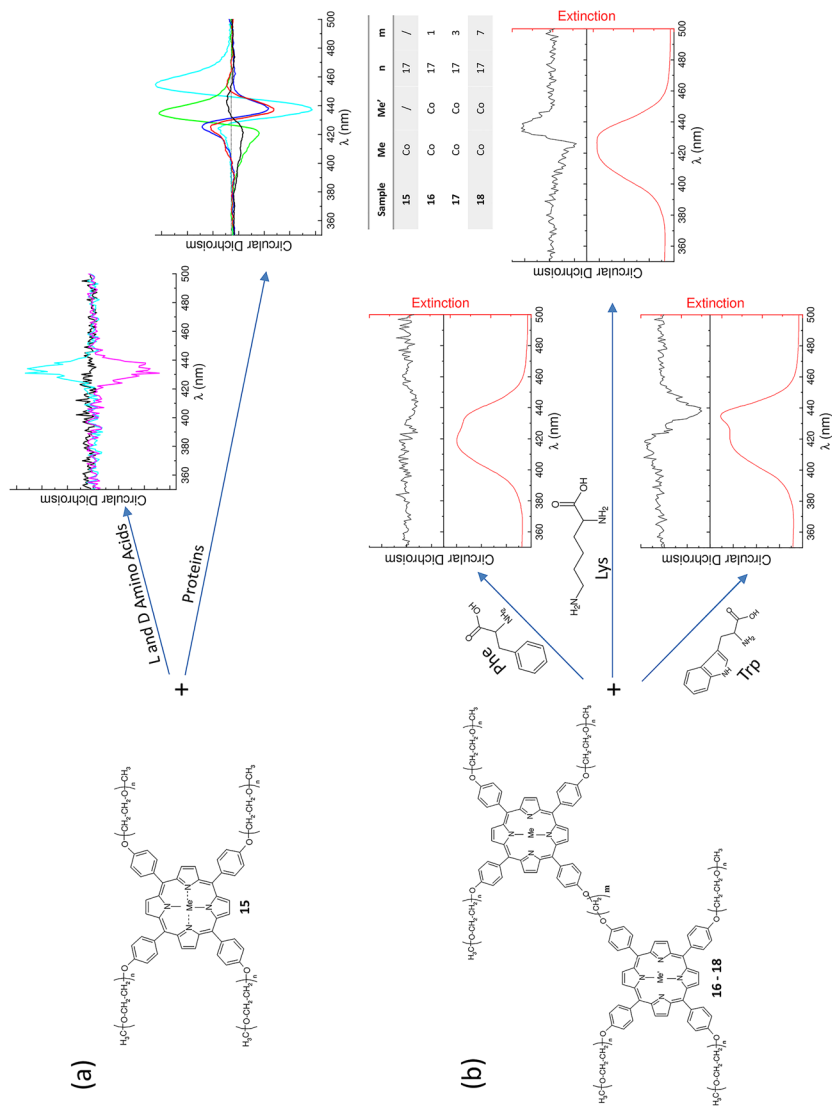


Fig. 7 a,b Examples of induced circular dichroism (ICD) profile of PEGylated porphyrin derivatives (samples **15–18**) upon binding with different proteins (**a**) or amino acids (**a and b**)

Fig. 8 Circular dichroism (CD) spectra of a PEGylated porphyrin derivative **8** in aqueous solution collected at different temperature gradient; *arrows* indicate the effect of increasing gradient strength on the CD bands

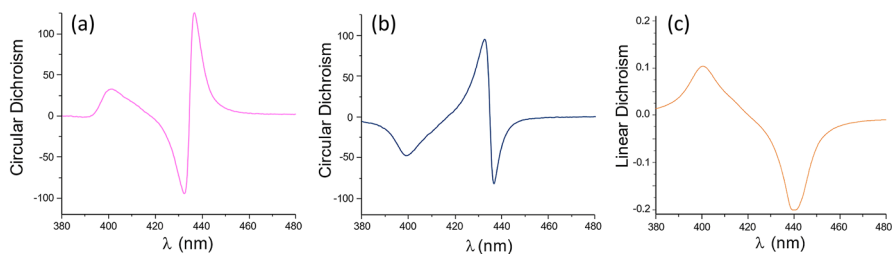
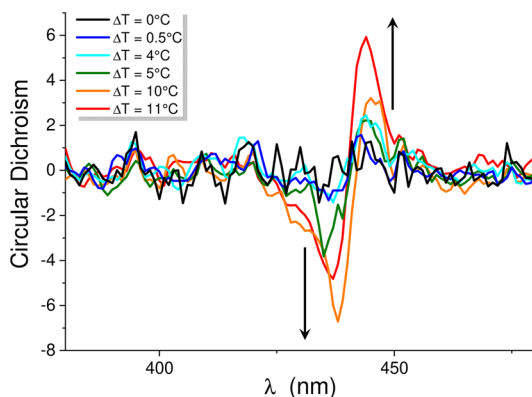


Fig. 9 **a,b** CD spectra of PEGylated porphyrin derivative **8** showing inversion of the CD signal under inversion of the thermal gradient: traces in **a** and **b** are examples recorded under opposite directions of the thermal force. **c** Corresponding linear dichroism (LD) maintains the same sign under an opposite sense of the perturbation

by a thermal gradient typically not larger than $0.1\text{ }^{\circ}\text{C}/\text{cm}$) causes chiral deformation of the aggregates through the thermophoresis phenomenon [56, 57].

This local deformation of the aggregates is traduced into a non-zero CD signal whose intensity depends on the thermal gradient strength (Fig. 8). Supramolecular chirality vanishes after the thermal gradient is switched off. It should be highlighted that, by applying the opposite sense perturbation, the sign of the induced chirality on aggregates is reversed (Fig. 9a,b).

A specific study found a correlation between the supramolecular aggregates size and appearance of the CD signal [58], showing that only mesoscopic sized aggregates behave as “flags”, intercepting the flows generated by thermal gradients and responsible for the chiral supramolecular deformations revealed as CD signal. Smaller aggregates instead change their orientation, which is revealed as a linear dichroism (LD) signal.

The occurrence of asymmetric local deformations of the aggregates can be related directly to the absence of electrostatic interactions between adjacent porphyrins and definitely suggests that the emergence of unexpected chirality originates from some uncontrolled asymmetric external force.

Large anisotropic aggregates are also inclined to align under the effect of the perturbation, so displaying a LD. Figure 9c displays the LD profiles collected under the thermal gradient; unlike the observed CD signals, they are independent of the chiral sense of the perturbation.

In the presence of strong LD, a fictitious CD signal can also appear (cross-talk effects). In order to estimate the contribution of alignment correctly, and to avoid misleading interpretation, measurement of LD is essential. For PEGylated porphyrins forming sub-micrometric fractal-like aggregates, for example, the cross-talk effect exists but it remains small for the J-band (typically less than 5%) [56]; for the H-band, on the other hand, it is so significant as to produce visible distortions into the corresponding CD signal (Fig. 9a and b illustrate an example). This means that the efficient exciton coupling of the transition dipole moments in the slipped arrangement overcomes the effect of alignment.

5 Photosensitizer Properties and Potentiality in Cancer Therapy and Diagnostic Imaging

Porphyrins are known as efficient photosensitizers for applications in the photodynamic therapy (PDT) of solid tumors to cause cell death locally using a treatment based on the use of porphyrins in combination with a light source and the presence of oxygen. Indeed, porphyrins excited with visible light (typically within the Q-bands region of the absorption spectrum) are able to de-activate the excited singlet level, besides through emission of fluorescence, by intersystem crossing to the triplet state with high quantum yield. This level has the proper energy and relatively long lifetime to promote, by energy transfer, the molecular oxygen from the triplet to singlet state or to form free radicals from biological substrates (Fig. 10). Free radicals and singlet oxygen are all very reactive species, thus causing oxidative stress to cells until their death.

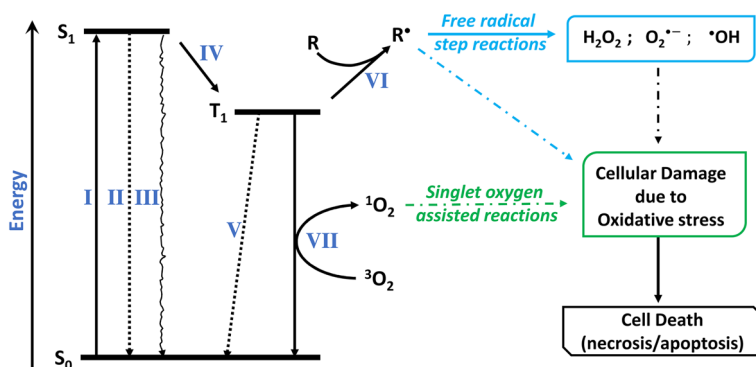


Fig. 10 Schematic representation of the oxidation reactions triggered by photo-excited porphyrins: *I* absorption, *II* fluorescence, *III* internal conversion, *IV* intersystem crossing, *V* phosphorescence, *VI* formation of free radicals by energy transfer (*R* biological substrate), *VII* singlet oxygen formation by energy transfer

In this context, the attachment of PEG chains offers more solutions not only in terms of solubility in water, but also for modulating the amphoteric character involved in interactions with cell membranes. In the latter case, moreover, the uncharged species are an optimum strategy to improve the crossing of membranes and to gain access to cell compartments.

Many studies highlighted that the dark cytotoxicity of PEGylated porphyrins is negligible or very low in the working concentration range [25, 59–61] and significantly lower than the parent porphyrin at the same concentration [35], especially the metal-free species.

According to the literature, on the other hand, photoinduced toxicity in cells can depend on different factors. First among these factors is the quantum yield of production of reactive species under irradiation, and, for singlet oxygen, it can be evaluated directly by measuring its phosphorescence [18]. However, it is generally estimated by indirect methods: in aqueous solution from the decrease of the optical density of an added specific molecule in the presence of the PEGylated porphyrin, with reference to a known system [61–63], and *in vitro* from the measurement of the cell viability before and after irradiation [25, 60].

Another important factor is the cellular uptake of these compounds, which was found to depend on the number and length of PEG chains, and on the nature of the coordinated metal ion and the axial ligand when present [25, 64]. This is ascribable to the achievement of the best balance between the hydrophilic and hydrophobic character of the whole molecule, the former avoiding extended aggregation, the latter guaranteeing the interaction with cell membranes. Although PEGylated porphyrins do not seem to get into the cell nucleus, their uptake is rather efficient (even in the presence of a time dependence related to hydrophilicity) and their localization occurs mainly in lysosomes and the endoplasmic reticulum [32–35].

Therefore, published works show that PEGylated porphyrins retain their photosensitizer properties, exploitable in PDT, and have numerous advantages with respect to their parent porphyrins, including increased bioavailability, decreased immunogenicity, and optimized pharmacokinetics.

Internalization, however, can be improved to further enhance PDT efficacy by using liposomes or vesicular structures as carriers or by forming inclusion complexes (for example, with modified cyclodextrins [62]).

Indeed, although also in this case the interaction with liposome depends on the number and length of PEG chains [30, 65], the tendency to self-aggregation of porphyrins decreases in the presence of liposomes because they are solubilized in the bilayer [35]. In particular, the chromophore stays in the hydrophobic interior of the bilayer, whereas the PEG chains remain in the outer surface exposed to water and can further screen the molecules from the solvent. Some fluorescence studies have suggested such an occurrence because isolation of the dye from contact with water avoids quenching by collision with solvent molecules [30, 36].

For the more soluble species (higher PEG chain length), dark toxicity is not improved significantly by entrapment within liposomes, but the intracellular distribution consequent to uptake can change drastically [66]. Localization in different cell compartments may, in turn, influence the mode of cell death after irradiation.

The usefulness of PEGylated porphyrins extends to tumor diagnostics, progression and response to therapy through imaging. It has been demonstrated that changes in tissue oxygenation can be evaluated *in vivo* and in real time by measuring the phosphorescence quenching of specific metal porphyrin derivatives. Their hydrophobic dendritic structure protects the porphyrin core, whereas the PEG branches provide water solubility and prevent interactions with biological macromolecules [24, 67].

The combination of PDT with other therapeutic approaches, such as chemo-, gene- and photothermal-therapy, or with diagnostics, can also be achieved by proper functionalization of the PEGylated porphyrin or modification of the platform used for delivery [62, 68, 69]. As a recent example, a PEGylated penta-porphyrinic system has been synthesized in order to mix the features of different porphyrin platforms and obtain a stimuli-responsive tool suitable for PDT and/or nanosurgery, depending on the wavelength of the light used for triggering (Fig. 11) [70].

6 Potential as Optical Sensors and Catalysts

PEGylation leaves most properties of porphyrins unaffected, so that their optical response and electrochemical activity are well suited for use in catalysis and sensing applications, for which reaction and detection are often expected to take place in water.

Unbound, bound to a solid substrate or embedded into synthetic membranes [27, 71, 72], PEGylated porphyrins can be exploited for pH sensing purposes in water solution (Fig. 12). The covalent binding to the substrates takes place on macro- and/

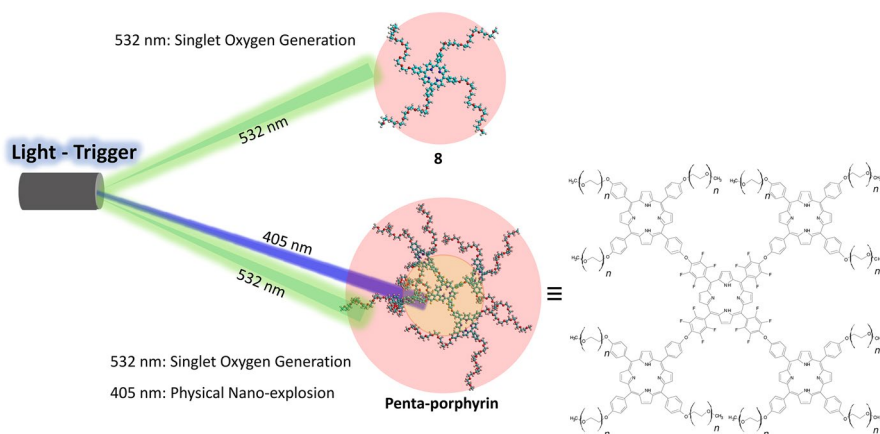


Fig. 11 *Left* Schematic representation of the different stimuli-response mechanisms of the PEGylated porphyrin systems: *green light* produces singlet oxygen due to the excitation of the PEGylated moieties; *blue light* induces physical nano-explosions of Penta-porphyrin system. *Right* Chemical structure of the Penta-porphyrin system ($n=9$)

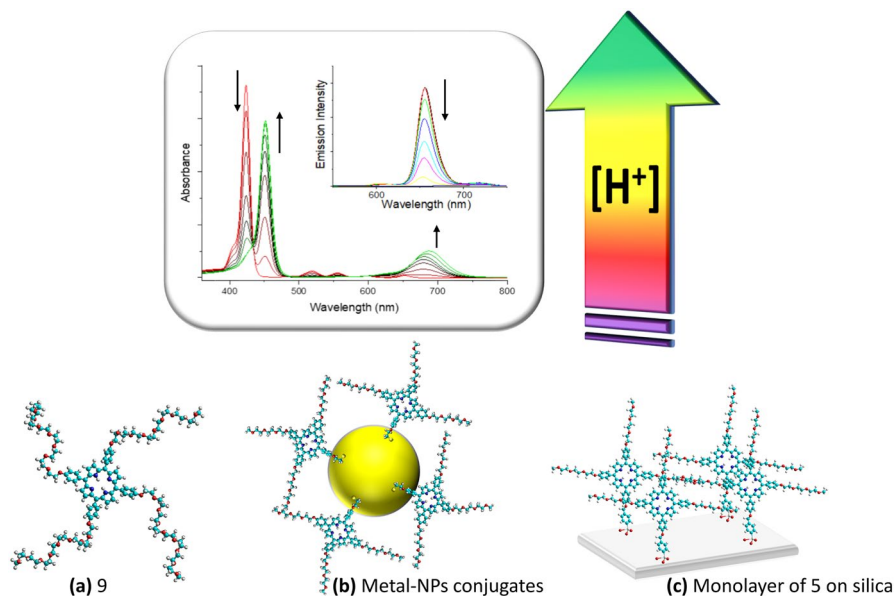


Fig. 12 Top Ultraviolet-visible (UV–Vis) (inset fluorescence) spectroscopic variations due to the increase of acid concentration. Bottom Schematic representation of PEGylated porphyrin derivatives with pH-sensitive properties when unbound (a) or bound to NPs (b) or silica surface (c)

or nano-sized substrates, without altering the optical properties of the porphyrin core.

The main advantage of solid optical pH sensors is the easy removal of the probe from the analyzed environment—the kind and size of the substrate determining various applications in biological and/or analytical fields. The measure is based on the absorbance signal of porphyrin bound to a macro-sized support; in particular, protonated porphyrin exhibits a significant red-shifted Soret band (with a deep modification of Q-bands) with respect to neutral porphyrin [73, 74]. A similar spectroscopic feature has been also verified in PEGylated porphyrin bonded to metal nanoparticles; such a nano-support makes the hybrid system suitable for pH sensing applications also in biological environments. Lowering of the pH induces quenching of the fluorescence emission signal, and because the fluorimetric approach is generally more sensitive than the comparable colorimetric (absorbance) mode, it represents an even more reliable signal to monitor pH variations [69, 75, 76].

PEGylated porphyrin derivatives do not lose their spectroscopic response to acidity variations in organic environments (i.e., fuels). In particular, the red-shift of the Soret band and the deep modification of Q-bands (the decrease of the four Q-bands, typical of free porphyrin, and the growth of a new red-shifted Q-band) occurs when acid species are present in an organic environment. Moreover, it also induces fluorescence emission quenching and/or formation of a new red-shifted emission band as a function of the excitation wavelength. These features also make the multi-solvent soluble PEGylated porphyrin a potential optical-sensor tool in both organic and aqueous environments [77].

PEGylated porphyrins can also act as electron donor or acceptor upon photoexcitation, when supramolecular binding occurs with a wide variety of molecules, aggregates and substrate. The donor/acceptor system formed is called a “ground-state complex”, because the ground-state levels of both species are involved, with significant superposition of the electronic orbitals that can be permanent (static interaction) or transient (during photoexcitation). In the former case, the complex is formed via various kinds of supramolecular interactions, in the latter, the transient electrostatic attraction is due to the electron transfer and it ceases after the fast charge recombination process.

The effect of such an interaction on the absorption spectrum of porphyrin consists in an evident red-shift and amplitude decrease of the Soret band. Occurrence of the electron transfer process also gives rise to significant changes in the emission properties of the dye. Indeed, the singlet excited state of porphyrin is fast deactivated by electron transfer and consequent charge recombination, resulting in significant fluorescence quenching.

The study of the photophysical properties related to these processes in supramolecular complexes is of fundamental importance both in terms of knowledge of the interaction or binding mechanisms and for optimizing such systems for the required applications from sensor to energy conversion devices. Also in this case PEGylation of porphyrins represents an interesting challenge, by avoiding the ionic contribution of chargeable groups.

Thus, the potential of PEGylated porphyrins as turn-off fluorescent probes becomes clear, and has been studied for the determination of pollutants or toxic species dissolved in water [78]. Indeed, under appropriate concentration conditions, the inverse of fluorescence intensity is proportional to the amount of target species (pollutant or other), thus allowing its presence to be determined and its concentration estimated.

The sensitivity of the fluorescent sensor can be improved (especially at low concentration of target) by a turn-on fluorescence approach, i.e., based on a fluorescence increase upon interaction with the target. This is possible by building up, via electron transfer, no more emitting supramolecular complexes, which are stable until an added species, competing with porphyrin, perturbs the supramolecular interaction and promotes the complex dissociation into the original components. Consequently, fluorescence of porphyrins, free again in the bulk, is turned on (Fig. 13) [79].

The presence of metal atoms within the porphyrin core of PEGylated porphyrin derivatives has been used to tune some sensing capability of these systems. It should be noted that the interaction between metal atoms and porphyrin core induces spectroscopic shifts in the Soret band of the metal porphyrin, attributed to $\pi-\pi^*$ excitations [48]. Moreover, metal induces enhanced intersystem crossing to the triplet state, resulting in fluorescence emission quenching. Among several metal-PEGylated porphyrins, cobalt-PEGylated porphyrin exhibits the capability of selectively binding aromatic amino acids due to the hydrophobic effect of the porphyrin core and the coordination bond with the metal atom [80]. In particular, the binding of aromatic amino acids occurs due to the interaction between amino groups of the guest molecule and the central metal atom, but also due to the stacking interaction between aromatic rings of porphyrins and aromatic guests. The formation of this

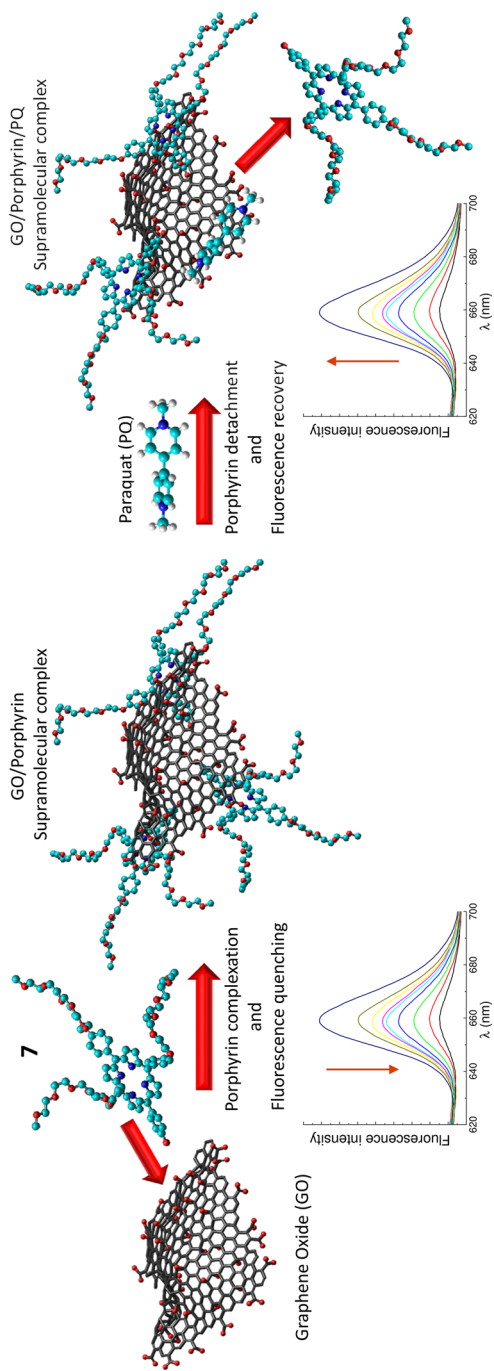


Fig. 13 Schematic representation of the fluorescent sensor based on supramolecular interactions: the graphene oxide/PEGylated porphyrin 7 complex no longer emits due to the electron transfer mechanism; the interaction with a competitor species (i.e., Paraquat) promotes complex dissociation; detachment of the PEGylated porphyrin, which moves from the complex to the bulk solution, restores porphyrin emission [79]

complex through a static interaction was confirmed by the variation in porphyrin fluorescence anisotropy behavior, as evidenced by the slowdown of the rotational dynamics with respect to that of the free cobalt-porphyrin system (Fig. 14). Moreover, fluorescence anisotropy measurements also suggested the formation of a sandwich-like complex where two porphyrinic moieties surround suitable amino acids [48].

The occurrence of chirality induction on PEGylated porphyrin by chiral species, shown in the section on [Chirality Induction](#), can be also exploited to recognize selectively globular proteins in water environments, through selective interactions with amino acids residues [49] present on the protein surface (Fig. 14). Note that, due to the uncharged nature of PEGylated porphyrin derivatives, the native protein structure is not altered by interaction with metal-PEGylated porphyrin [49].

Another aspect, related to the important role played by porphyrins in nature and for applications, concerns their catalytic and photocatalytic properties. These are influenced in different ways by the covalent linkage of PEG chains, enabling the application of PEGylated porphyrin derivatives in different fields such as organic reaction conversion and environmental remediation.

As far as the porphyrin-catalyzed oxidation reactions are concerned, the goal is manifold, encompassing the achievement of useful compounds through cheaper pathways and by starting from more readily available substances [81]. Undoubtedly, the PEG functionalization of the porphyrin core influences the solubility of the system and simplifies catalyst removal and recycling, including in photo-oxidation reactions [82]. PEGylated ruthenium and manganese metalloporphyrin derivatives have been employed in hydrocarbon oxidation [83, 84], exploiting the PEG chains to improve catalyst efficiency in aqueous media [85]. Moreover, nanoparticles of PEGylated manganese-porphyrin derivative, prepared through combined self-assembly and cross-linking, have been used for catalytic oxidation of cyclohexene in

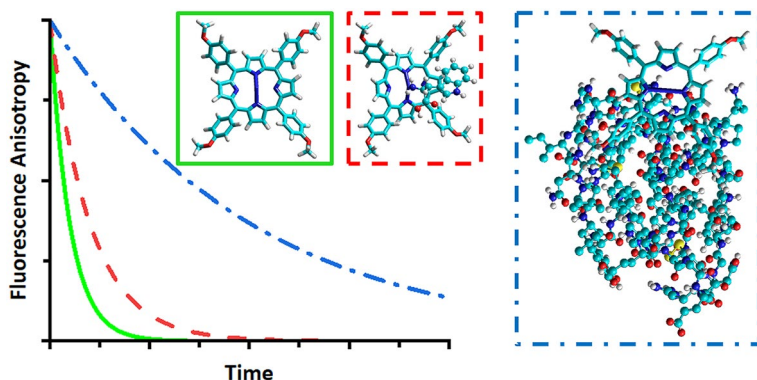


Fig. 14 The time dependence of the fluorescence anisotropy is related to the characteristic time of the dye rotational diffusion. This characteristic time changes when binding with another species occurs; it slows down more and more with increasing size of the species. Here the slowing down is displayed for the PEGylated derivative **15** (solid line) and upon binding with an amino acid (dashed line) or with a protein (dot-dashed line), as examples. For the sake of clarity, PEG chains in porphyrin peripheral positions are not shown

aqueous media, exhibiting higher catalytic activity than the bare metal porphyrin in organic solvents [86].

Other iron porphyrin derivatives have been investigated as electrocatalysts in CO₂ reduction, by exploiting the stability of the iron–carbon adduct. Recently, PEGylation of the porphyrin unit has improved the catalytic activity of the system in electrochemical CO₂ reduction, providing a second coordination sphere that enables a concerted mechanism involving the PEG chains and water molecules [87].

Applications of PEGylated porphyrins in environmental remediation have also been reported. Complex amphiphilic nanosystems containing a PEG-supported manganese-porphyrin have been used for chlorophenol photocatalytic degradation in water environments [88]. On the other hand, a metal-free PEGylated derivative, intercalated within a nanoclay, was investigated in adsorption and photooxidation of phenol in water [89]. All methods are based on the ability of porphyrins to generate singlet oxygen under suitable light irradiation, inducing the oxidation of compounds in their proximity.

Porphyrin derivatives are also involved as catalysts in many biological processes such as photosynthesis and oxygen transport [90, 91]. Due to their biocatalytic features, research has been conducted to exploit them in laboratory-scale biocatalytic reactions. PEGylated porphyrin derivatives are more stable catalysts than oxidoreductase enzymes in polymerization reactions of aniline- and phenol-based monomers [92].

7 Conclusions and Perspectives

Porphyrins certainly represent a vast and thoroughly studied variety of dyes, but they also present some drawbacks that limit their potential use and application. One such limit is surely the poor solubility in water of some non-ionic species. Thanks to the relatively easy functionalization of peripheral groups, solubility in water is achieved mostly by linking PEG chains. The class of molecules obtained, PEGylated porphyrins, have turned out to have interesting properties for basic science and to be very versatile and promising compounds in numerous application fields. Interest in PEGylated porphyrins has been growing in the last two decades and the subject is widespread in many scientific areas. Nevertheless, each published work is necessarily circumscribed into the ambit of its specific area, so that, to the best of our knowledge, an overview of the properties and potentiality of PEGylated porphyrins was lacking. This review aimed to recap and discuss the results of recent publications devoted to the study of non-ionic PEGylated porphyrin in aqueous solutions, by grouping them under different headings according to the goal of the research. The literature indicates that these macromolecular architectures are fruitful systems for investigating self-assembly phenomena, exciton coupling, resonance effects and supramolecular binding with various target species, in the absence of the electrostatic contribution. No less important, they also contribute to the comprehension of chirality induction and the role of weak external physical perturbation in the debated and stimulating symmetry breaking phenomenon.

Regarding applications, the research works span a vast range of topics, from use in cancer therapy and diagnostics to sensors and catalysis. From the huge amount of data it is clear that these systems possess many of the properties required by these related fields, but much work still needs to be done in order to achieve specificity and selectivity towards targets. Interesting perspectives surely concern urgent environmental problems, in particular green chemistry and the detection of pollutants, but strong expectations are addressed also to nanomedicine and personalized medicine. Indeed, proper functionalization of non-ionic PEGylated porphyrins could merge the ability of internalization in different cell compartments and the recognition of specific cells and tissues, with the aim of minimizing side effects and excessive toxicity of the current therapies. In addition, along with the rapid growth of more and more sensitive and accessible instrumentations, uncharged PEGylated porphyrins could improve diagnostic techniques for early therapeutic approaches.

Among all the opportunities opened, our future research will be devoted to the development of innovative multifunctional materials based on PEGylated porphyrins anchored, as a side-chain, on suitable polymers. The aim is to improve the properties of hybrid nanocomposites based on semiconductor oxide (e.g., titanium dioxide) nanoparticles, with a focus on photocatalytic and sensing properties. Indeed, with proper efficiency, such materials could be used in energy-sustainable methods to support indoor air or water depollution in human environments in which fresh air or water replacement is not easy to obtain (for example, in underground or out-of-orbit laboratories).

Another aspect that will also be explored is the in-depth use of this class of porphyrin in the nanomedicine field, after suitable modification with active targeting agents and/or drugs, thanks to the multi-faceted capability of these systems to act as theranostic agents.

Finally, some attention has been devoted very recently to the phosphorescence properties of platinum or palladium porphyrin derivatives for applications in oxygen and small molecule detection. Optical oxygen sensors, in fact, present good detection accuracy, promising anti-interference ability and easy miniaturization, which has interesting perspectives in the environmental monitoring of water quality, but also in clinical approaches and medical diagnostics for tissue health. In this context, systematic studies on PEGylated porphyrin derivatives are very few and surely deserve more insight.

In summary, the future of this class of porphyrin derivatives is still challenging and much of their potential remains unexplored, and thus they are all the more deserving of the attention of researchers working in different scientific and applicative areas.

Funding This research was partially funded by the University of Catania (PIAno di inCEntivi per la Ricerca di Ateneo, PIACERI–Linea 2) and by MIUR with PRIN 2017 Prot. 2017YJMPZN.

Declarations

Conflict of interest The authors declare no conflicts of interest.

References

1. Min Park J, Lee JH, Jang W-D (2020) *Coord Chem Rev* 407:213157
2. Mukhopadhyay RD, Kim Y, Koo J, Kim K (2018) *Acc Chem Res* 51:2730–2738
3. Chen Y, Li A, Huang Z-H, Wang L-N, Kang F (2016) *Nanomaterials* 6:51
4. Bodedla GB, Huang J, Wong W-Y, Zhu X (2020) *ACS Appl Nano Mater* 3:7040–7046
5. Bodedla GB, Li L, Che Y, Jiang Y, Huang J, Zhao J, Zhu X (2018) *Chem Commun* 54:11614–11617
6. Luciano M, Brückner C (2017) *Molecules* 22:980
7. Hayashi T, Aya T, Nonoguchi M, Mizutani T, Hisaeda Y, Kitagawa S, Ogoshi H (2002) *Tetrahedron* 58:2803–2811
8. D'Urso A, Mammana A, Balaz M, Holmes AE, Berova N, Lauceri R, Purrello R (2009) *J Am Chem Soc* 131:2046–2047
9. Sandland J, Malatesti N, Boyle R (2018) *Photodiagn Photodyn Ther* 23:281–294
10. Paolesse R, Nardis S, Monti D, Stefanelli M, Di Natale C (2016) *Chem Rev* 117:2517–2583
11. Martynov AG, Safonova EA, Tsivadze AY, Gorbunova YG (2019) *Coord Chem Rev* 387:325–347
12. Qi Z-L, Cheng Y-H, Xu Z, Chen M-L (2020) *Int J Mol Sci* 21:5839
13. Gouterman M (1961) *J Mol Spectrosc* 6:138–163
14. Gouterman M (1959) *J Chem Phys* 3:1139–1161
15. Wang F, Chen L, Zhu J, Hu X, Yang Y (2021) *Micromachines* 12:281
16. Li X, Roussakis E, Cascales JP, Marks HL, Witthauer L, Evers M, Manstein D, Evans CL (2021) *J Mater Chem C* 9:7555–7567
17. Monash A, Marciano D, Colvin A, Fass R, Dvash Y, Rosen O (2021) *Talanta* 224:121927
18. Ceroni P, Lebedev AY, Marchi E, Yuan M, Esipova TV, Bergamini G, Wilson DF, Busch TM, Vinogradov SA (2011) *Photochem Photobiol Sci* 10:1056–1065
19. Huang H, Song W, Chen G, Reynard JM, Ohulchanskyy TY, Prasad PN, Bright FV, Lovell JF (2014) *Adv Healthc Mater* 3:891–896
20. Kasha M (1963) *Radiat Res* 20:55–70
21. Pasternack RF, Schaefer KF, Hambright P (1994) *Inorg Chem* 33:2062–2065
22. Pasternack R, Collings P (1995) *Science* 269:935–939
23. Micali N, Villari V, Mineo P, Vitalini D, Scamporrino E, Crupi V, Majolino D, Migliardo P, Venuti V (2003) *J Phys Chem B* 107:5095–5100
24. Lebedev AY, Cheprakov AV, Sakadžić S, Boas DA, Wilson DF, Vinogradov SA (2009) *ACS Appl Mater Interfaces* 1:1292–1304
25. Sibirian-Vazquez M, Jensen TJ, Vicente MGH (2007) *J Photochem Photobiol B* 86:9–21
26. Hou Z, Dehaen W, Lyskawa J, Woisel P, Hoogenboom R (2017) *Chem Commun* 53:8423–8426
27. Thyagarajan S, Leiding T, Årsköld SP, Cheprakov AV, Vinogradov SA (2010) *Inorg Chem* 49:9909–9920
28. Crupi V, Majolino D, Migliardo P, Venuti V, Micali N, Villari V, Mineo P, Vitalini D, Scamporrino E (2003) *J Mol Struct* 651–653:675–681
29. Crupi V, Giordano R, Majolino D, Migliardo P, Venuti V, Micali N, Villari V, Mineo P, Vitalini D, Scamporrino E (2003) *Mol Phys* 101:1517–1526
30. Nawalany K, Kozik B, Kepczynski M, Zapotoczny S, Kumorek M, Nowakowska M, Jachimaska B (2008) *J Phys Chem B* 112:12231–12239
31. Villari V, Mineo P, Scamporrino E, Micali N (2012) *Chem Phys* 409:23–31
32. Purushothaman B, Choi J, Park S, Lee J, Samson AAS, Hong S, Song JM (2019) *J Mater Chem B* 7:65–79
33. Cheng L, Jiang D, Kamkaew A, Valdovinos HF, Im H-J, Feng L, England CG, Goel S, Barnhart TE, Liu Z, Cai W (2017) *Adv Funct Mater* 27:1702928
34. Chung CY-S, Fung S-K, Tong K-C, Wan P-K, Lok C-N, Huang Y, Chen T, Che C-M (2017) *Chem Sci* 8:1942–1953

35. Nawalany K, Rusin A, Kępczyński M, Mikhailov A, Kramer-Marek G, Śnietura M, Połtowicz J, Krawczyk Z, Nowakowska M (2009) *J Photochem Photobiol B* 97:8–17
36. Kępczyński M, Nawalany K, Jachimska B, Romek M, Nowakowska M (2006) *Colloids Surf B* 49:22–30
37. Wang J, Liu L, Yin L, Chen L (2018) *J Biomed Mater Res Part A* 106:2955–2962
38. Mandal AK, Sahin T, Liu M, Lindsey JS, Bocian DF, Holten D (2016) *New J Chem* 40:9648–9656
39. Villari V, Mineo P, Scamporrino E, Micali N (2012) *RSC Adv* 2:12989–12998
40. Pescitelli G, Gabriel S, Wang Y, Fleischhauer J, Woody RW, Berova N (2003) *J Am Chem Soc* 125:7613–7628
41. Spano FC (2010) *Acc Chem Res* 43:429–439
42. Mineo P, Spitaleri F, Scamporrino E (2013) *J Polym Sci Part A* 51:1428–1435
43. Scamporrino E, Mineo P, Vitalini D (2011) *Tetrahedron* 67:3705–3713
44. Yuan W, Chen X (2016) *RSC Adv* 6:6802–6810
45. Liu C, Li Y, Gao B, Li Y, Duan Q, Kakuchi T (2018) *Mater Sci Eng C* 82:155–162
46. Akhtar MA, Riaz S, Hayat A, Nasir M, Muhammad N, Rahim A, Nawaz MH (2017) *J Mol Liq* 225:235–239
47. Zhang T, Fang J, Tsutsuki H, Ono K, Islam W, Sawa T (2019) *Biol Pharm Bull* 42:1199–1206
48. Angelini N, Micali N, Mineo P, Scamporrino E, Villari V, Vitalini D (2005) *J Phys Chem B* 109:18645–18651
49. Mineo P, Micali N, Villari V, Donato MG, Scamporrino E (2012) *Chem Eur J* 18:12452–12457
50. Villari V, Mineo P, Micali N, Angelini N, Vitalini D, Scamporrino E (2007) *Nanotechnology* 18:375503
51. Scamporrino E, Mineo P, Dattilo S, Vitalini D, Spina E (2007) *Macromol Rapid Commun* 28:1546–1552
52. Ohno O, Kaizu Y, Kobayashi H (1993) *J Chem Phys* 99:4128–4139
53. Ribo JM, Crusats J, Sagués F, Claret J, Rubires R (2001) *Science* 292:2063–2066
54. Micali N, Engelkamp H, van Rhee PG, Christianen PCM, Scolaro LM, Maan JC (2012) *Nat Chem* 4:201–207
55. D’Urso A, Randazzo R, Lo Faro L, Purrello R (2010) *Angew Chem Int Ed* 49:108–112
56. Mineo P, Villari V, Scamporrino E, Micali N (2014) *Soft Matter* 10:44–47
57. Mineo P, Villari V, Scamporrino E, Micali N (2015) *J Phys Chem B* 119:12345–12353
58. Nicosia A, Vento F, Marletta G, Messina GML, Satriano C, Villari V, Micali N, De Martino MT, Schotman MJG, Mineo PG (2021) *Nanomaterials* 11:1673
59. Sibirian-Vazquez M, Jensen TJ, Vicente MGH (2007) *Bioconjugate Chem* 18:1185–1193
60. Nowakowska M, Nawalany K, Kępczyński M, Krawczyk Z (2009) *Macromol Symp* 279:132–137
61. Mineo P, Faggio C, Micali N, Scamporrino E, Villari V (2014) *RSC Adv* 4:19389–19395
62. Wang J, Liu L, Chen J, Deng M, Feng X, Chen L (2019) *Eur Polym J* 118:222–230
63. Obata M, Hirohara S (2016) *J Photochem Photobiol B* 162:324–331
64. Mewis RE, Savoie H, Archibald SJ, Boyle RW (2009) *Photodiagn Photodyn Ther* 6:200–206
65. Sholto A, Lee S, Hoffman BM, Barrett AGM, Ehrenberg B (2008) *Photochem Photobiol* 84:764–773
66. Nawalany K, Rusin A, Kępczyński M, Filipczak P, Kumorek M, Kozik B, Weitman H, Ehrenberg B, Krawczyk Z, Nowakowska M (2012) *Int J Pharm* 430:129–140
67. Esipova TV, Karagodov A, Miller J, Wilson DF, Busch TM, Vinogradov SA (2011) *Anal Chem* 83:8756–8765
68. Spagnul C, Alberto R, Gasser G, Ferrari S, Pierroz V, Bergamo A, Gianferrara T, Alessio E (2013) *J Inorg Biochem* 122:57–65
69. Mineo P, Abbadessa A, Mazzaglia A, Gulino A, Villari V, Micali N, Millesi S, Satriano C, Scamporrino E (2017) *Dyes Pigment* 141:225–234
70. Nicosia A, Vento F, Satriano C, Villari V, Micali N, Cucci LM, Sanfilippo V, Mineo PG (2020) *ACS Appl Nano Mater* 3:1950–1960
71. Worlinsky JL, Halepas S, Ghandehari M, Khalil G, Brückner C (2015) *Analyst* 140:190–196
72. Gulino A, Mineo P, Fragalà I (2006) *J Phys Chem C* 111:1373–1377
73. Gulino A, Mineo P, Bazzano S, Vitalini D, Fragalà I (2005) *Chem Mater* 17:4043–4045
74. Gulino A, Mineo P, Scamporrino E, Vitalini D, Fragalà I (2006) *Chem Mater* 18:2404–2410
75. Mineo PG, Abbadessa A, Rescifina A, Mazzaglia A, Nicosia A, Scamporrino E (2018) *Colloids Surf A* 546:40–47
76. Nicosia A, Abbadessa A, Vento F, Mazzaglia A, Mineo PG (2021) *Materials* 14:2764

77. Mineo PG, Vento F, Abbadessa A, Scamporrino E, Nicosia A (2019) *Dyes Pigm* 161:147–154
78. Worlinsky JL, Halepas S, Brückner C (2014) *Org Biomol Chem* 12:3991–4001
79. Micali N, Mineo P, Vento F, Nicosia A, Villari V (2019) *J Phys Chem C* 123:25977–25984
80. Angelini N, Micali N, Villari V, Mineo P, Vitalini D, Scamporrino E (2005) *Phys Rev E* 71:21915
81. Neves CMB, Tomé JPC, Hou Z, Dehaen W, Hoogenboom R, Neves MGPMS, Simões MMQ (2018) *ChemCatChem* 10:2804–2809
82. Benaglia M, Danelli T, Fabris F, Sperandio D, Pozzi G (2002) *Org Lett* 4:4229–4232
83. Benaglia M, Danelli T, Pozzi G (2003) *Org Biomol Chem* 1:454–456
84. Zhang J-L, Che C-M (2002) *Org Lett* 4:1911–1914
85. Zhang J-L, Huang J-S, Che C-M (2006) *Chem Eur J* 12:3020–3031
86. Xu LQ, Chen JC, Qian SS, Zhang AK, Fu GD, Li CM, Kang E-T (2015) *Macromol Chem Phys* 216:417–426
87. Chaturvedi A, Williams CK, Devi N, Jiang JJ (2021) *Inorg Chem* 60:3843–3850
88. Cho KY, Kim H-J, Do XH, Seo JY, Choi J-W, Lee S-H, Yoon HG, Hwang SS, Baek K-Y (2018) *Res Chem Intermed* 44:4663–4684
89. Drozd D, Szczubiałka K, Kumorek M, Kepczynski M, Nowakowska M (2014) *J Photochem Photobiol A* 288:39–45
90. Falk JE, Smith KM (1975) *Porphyryns and metalloporphyryns*. Elsevier, Amsterdam
91. Grimm B, Porra RJ, Rüdiger W, Scheer H (2006) *Chlorophylls and bacteriochlorophylls: biochemistry, biophysics functions and applications*. Springer, Dordrecht
92. Nagarajan S, Nagarajan R, Tyagi R, Kumar J, Bruno FF, Samuelson LA (2008) *J Macromol Sci Part A* 45:951–956

Publisher's Note Springer Nature remains neutral with regard to jurisdictional claims in published maps and institutional affiliations.